Regulating ankyrin dynamics: Roles of sigma-1 receptors

Teruo Hayashi and Tsung-Ping Su*

Ankyrin is a cytoskeletal adaptor protein important cellular functions, including Ca^{2+} efflux at inositol 1,4,5-trisphos-phate receptors (IP_3R) on the ER. sigma-1 receptors (Sig-1R), unique ER proteins that bind certain steroids, neuroleptics, and psychotropic drugs, form a trimeric complex with ankyrin B and IP_3R type 3 (IP_3R-3) in NG-108 cells. trimeric complex could be coimmunoprecipitated by antibodies against anY. Sig-1R agonists such as pregnenolone sulfate and cocaine caused dissociation of an ankyrin B isoform (ANK 220) from IP_3R-3.

This effect caused by Sig-1R agonists was blocked by a Sig-1R antagonist. The degree of dissociation of ANK 220 from IP_3R-3 caused by Sig-1R ligands correlates excellently with the ligands' efficacies in potentiating the bradykinin-induced increase in cytosolic free Ca^{2+} concentration. Immunocytohistochemistry showed that Sig-1R, ankyrin B, and IP_3R-3 are colocalized in NG-108 cells in perinuclear areas and in regions of cell-to-cell communication. Sig-1R and associated ligands may play important roles in cells by controlling the function of cytoskel-etal proteins and that the Sig-1R/ANK220/IP_3R-3 complex regulat-ing Ca^{2+} signaling may represent a site of action for neurosteroids and cocaine.

Ankyrins are a family of cytoskeletal adaptor proteins that interconnect membrane proteins with the spectrin-based cytoskeleton (1, 2). Ankyrins are present in specialized areas of plasma membranes and also on endoplasmic reticulum (ER) and Golgi complex

Thus, ankyrin controls several cellular functions, such as vesicle transport, protein trafficking, ion channel clustering on axons, and intracellular sorting of Ca^{2+} homeostasis proteins (3–6), as well as the structural support for membrane. It is also known that ankyrin affects Ca^{2+} efflux from intracellular organelles by interacting with inositol 1,4,5-trisphosphate receptors (IP_3R) (7, 8). Additionally, it was suggested that as yet unidentified binding partners for ankyrins exist to complement ankyrin actions at the ER (6).

Sigma-1 receptors (Sig-1R), were later found to bind several classes of ligands, including neurosteroids, neuroleptics, dextrobenzomorphans, and psychostimulants such as cocaine Sig-1R exhibit unique distribution patterns in the brain and have been demonstrated to play important roles in learning and memory in animal models of amnesia and in cocaine-induced behavioral alterations. Sig-1R also exist in endocrine and peripheral systems.

For example, Sig-1R ligands affect intrasynaptosomal free Ca^{2+} level and protein phosphorylation in rat brain (24). Sig-1R ligands also affect the *N*-methyl-D-aspartate-induced Ca^{2+} signaling in rat primary neurons (25, 26). Exposure of myocardiac cells to Sig-1R ligands affects contractility and Ca^{2+} influx of the cells (27, 28). Further, we have shown recently that Sig-1R reside in close proximity to IP_3R at the ER (29) and can affect intracellular Ca^{2+} signaling thereof (30).

Because ankyrin is known to play important roles in regulating Ca^{2+} signaling at IP_3R on the ER (7, 8) and because Sig-1R may reside close to IP_3R at the ER (29) affecting Ca^{2+} signaling thereof (30), a possibility exists that the action of Sig-1R may be related to ankyrin. The present study examined this possibility.

Cell Culture and Cloning of Sig-1R from NG-108 Cells. Culture of NG-108 cells was performed as described (30). Standard cloning procedures were followed for the cloning of Sig-1R in NG-108 cells. Briefly, the extracted total RNA of the cells was treated with DNase I and reverse transcribed with random hexamer priming (CLONTECH). By using the products as template, PCR was performed by using 5′-CCAGGCTGCCCGCT-3′ as the sense primer and 5′-GTGAGTGCATGATCTTACAGTAC-3′ as the antisense primer. These sequences are 100% conserved between mouse Sig-1R (GenBank accession no. AF030198; sense base 5–18; antisense base 901–923) and rat Sig-1R (GenBank accession no. AF004218; sense base 22–35; antisense base 918–940). The PCR products were subcloned into the TA cloning vector (Invitrogen) and sequenced by the dideoxynucleotide chain termination method by using fluorescein donor dyes (Perkin–Elmer). Results indicated that the sequence of Sig-1R in NG-108 cells thus cloned is 100% identical to that of the rat Sig-1R as previously reported (31).

Subcellular Fractionation of NG-108 Cells. The subcellular fractionation was performed according to a previous report (32). Cells were washed twice with ice-cold PBS and harvested. All subsequent steps were carried out at 4°C. After centrifugation (400 × *g*, 5 min), cells were suspended in hypotonic TM buffer (10 mM Tris·HCl/1 mM $MgCl_2$/10 μg/ml aprotinin/1 mM PMSF; pH 7.4) and incubated for 20 min. The cell suspension was diluted with the same volume of TM buffer containing 0.5 M sucrose and cells disrupted by a Dounce homogenizer (20 strokes). The P1 fraction was obtained as a pellet after centrifugation at 900 × *g* for 5 min. The supernatants were centrifuged at 10,000 × *g* for 20 min to obtain the P2 fraction (the pellet). The resultant

IP_3R, inositol 1,4,5-trisphosphate receptor;(+)PTZ, (+)pentazocine; Sig-1R, sigma-1 receptors; $[Ca^{2+}]_{cyt}$, cytosolic free Ca^{2+} concen-tration; IP_3R-3, IP_3R type 3

supernatants were centrifuged at 105,000 × *g* for 60 min to yield the P3 fraction (the pellet). The P3 fraction was suspended in the TM buffer containing 1.35 M sucrose and further separated by centrifugation (SW28 rotor at 105,000 × *g*, 3 h, with the brake off) on discontinuous sucrose gradients (0.25 M, 0.8 M, 1.35 M, 2.1 M) into the P3L (layer between 0.8 M/1.35 M) and the P3H fractions (layer between 1.35 M/2.1 M). Each layer was collected separately and diluted with 6 vol of TM buffer without sucrose and recentrifuged at 150,000 × *g* for 3 h. The pellets were lysed and used for experiments. The subcellular fractions thus obtained were characterized by examining the relative enrichment of representative organelle markers in each fraction by Western blotting. In the present study, only the P3L fraction, containing the highest density of Sig-1R, was used to examine the dissociation of ANK220 from the subcellular fraction (see *Results*).

Immunoprecipitation and SDS/PAGE. Samples were dissolved in lysis buffer [10 mM Tris·HCl (pH 7.0)/150 mM NaCl/1% Nonidet P-40/0.5% deoxycholate/5 mM EDTA/1 mM EGTA/1 mM PMSF/10 μg/ml leupeptin/1 mg/ml benzamidine/15 μg/ml aprotinin/1 mM sodium orthovanadate] and sonicated (2 s × 3). After centrifugation, supernatants were subjected to immunoprecipitation or SDS/PAGE. For immunoprecipitation of IP_3R type 3 (IP_3R-3), freshly prepared samples containing 500 μg proteins were precleared and incubated with a mouse monoclonal anti-IP_3R-3 antibody (Transduction Laboratories, Lexington, KY) at a dilution of 1:50. Immunocomplexes were precipitated by protein A-Sepharose CL-4B beads (Amersham Pharmacia) with the addition of the anti-mouse IgG rabbit antibody (Jackson ImmunoResearch) to anchor the mouse IgG to the beads. When immunoprecipitants were to be used for Sig-1R Western blotting, however, the anti-mouse IgG rabbit antibody was omitted to avoid the masking of Sig-1R (30 kDa) by the predominant signal from the light chain of rabbit IgG. Polyclonal Sig-1R antibodies were raised in rabbits by using a peptide antigen corresponding to amino acids 144–165 of guinea pig Sig-1R (GenPept accession no. CAA91441). Protein lysates or immunoprecipitants were separated by SDS/PAGE and transblotted onto polyvinylidene difluoride membranes without methanol. For immunodetection, membranes were incubated with respective antibodies at the dilution of 1:1,500 for Sig-1R, 1:1,000 for IP_3R-3, and 1:150 for ankyrin B (mouse monoclonal; Oncogene Science) and visualized as described (30). The resultant protein bands were scanned digitally and densitometrically analyzed by a Macintosh computer-based analysis system (IMAGE, National Institutes of Health) (30). To examine the effects of different Sig-1R ligands on the coimmunoprecipitation of the protein complexes, the same procedures described before were followed (30). Briefly, before treatment of cells with Sig-1R ligands, cells in culture wells were deprived of FCS (which may contain endogenous steroids) by careful washings with Hanks' balanced salt solution containing 1% BSA. The cells remained cultured in the same buffer for at least 30 min before addition of Sig-1R ligands.

Confocal Microscopy of Cytosolic Free Ca^{2+} and Immunostaining. Cytosolic Ca^{2+} concentrations were measured as described elsewhere in great detail (30). Each experimental determination used a four-well FlexiPERM plate (Heraeus). The concentration of bradykinin used to elicit an increase in cytosolic Ca^{2+} concentration was 1 μM. An average of three to nine cells per culture well was examined in each determination, which always included a control well (30). In each determination, a similar treatment condition was never repeated in other wells, except occasionally the controls may have been repeated. In this report, data were obtained from an average of 5–14 determinations by examining an average total of 20–91 cells for each test drug. The mean values from multiple determinations are presented in the study (see Fig. 5 legend). Images of immunostaining were collected by using argon ion laser (488 or 543 nm) and long-pass barrier filter (520 or 590 nm). Sixteen images (512 × 512 pixels) were averaged and collected digitally by using Zeiss IMAGE software.

[^{3}H]IP_3-Binding Assay. The binding of [^{3}H]IP_3 (8 nM) to microsomes of NG-108 cells (100 μg) was assayed in 0.5 ml of ice-cold buffer containing 50 mM Tris·HCl (pH 8.0) and 1 mM EDTA. Tubes were incubated at 4°C with constant shaking. After 30 min, reactions were terminated by passing the tissue mixture through Whatman GF/B filters by means of a rapid single manifold filtration, followed by three washings with 5 ml of ice-cold buffer. The filters were presoaked with ice-cold buffer for 30 min before use. Filters were then soaked overnight in 6 ml of scintillation mixture (Poly Fluor; Packard, Meriden, CT) containing 0.8% (vol/vol) acetic acid. The radioactivity trapped on the filters was measured by using a liquid scintillation counter. Nonspecific binding was measured in the presence of 4 μM IP_3.

Immunostaining. Immunocytohistochemistry was performed on the 4% paraformardehyde-fixed cultured cells. The anti-Sig-1R IgG was affinity purified (AminoLink Kit; Pierce). Specificity was verified by using a preimmune serum and a preabsorbed Sig-1R antibody. Fixed cells were incubated with an anti-ankyrin B monoclonal antibody (1:200) and/or an anti-Sig-1R antibody (1:300) at 4°C for 24 h. For Sig-1R-ankyrin B double staining, Alexa 488 goat anti-rabbit IgG antibody or Alexa 590 goat anti-mouse IgG antibody, respectively (Molecular Probes), was used as the secondary antibody generating immunofluorescence. In Sig-1R-IP_3R-3 double staining, Alexa 590 goat anti-rabbit IgG antibody for Sig-1R, and FITC-conjugated anti-mouse IgG and Alexa 488 anti-FITC antibody for IP_3R-3 were used for immunofluorescence.

Drugs and Reagents. NG-108 cells were purchased from American Type Culture Collection. PRE084 was synthesized as described (33). (+)Pentazocine, (+)SKF-10047, and cocaine were from Division of Basic Research, National Institutes on Drug Abuse (Bethesda, MD). Pregnenolone sulfate, progesterone, and bradykinin were purchased from Research Biochemicals (Natick, MA). The anti-IP_3R type 1 antibodies were from Calbiochem and antiankyrin G antibodies from Oncogene Science. Other antibodies and their suppliers are: NADPH Cytochrome P450 reductase and bcl2 (StressGen Biotechnologies, Victoria, Canada); BiP/GRB78 and GM130 (Transduction Laboratories); Fas (Santa Cruz Biotechnology).

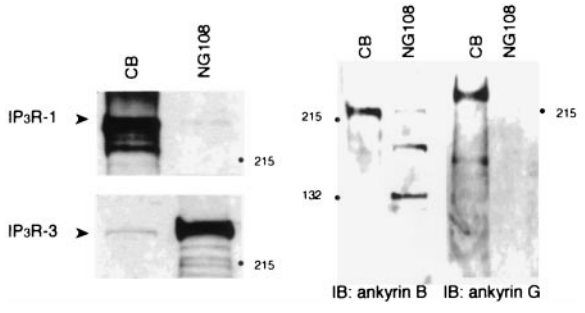

Fig. 1. Identification of IP_3R-3, ankyrin B in NG-108 cells. IP_3R-3 and ankyrin B exist in NG-108 cells. IP_3R type 1 (IP_3R-1) and ankyrin G were not detected. Positive controls of IP_3R type 1 and ankyrin G with the mouse cerebellum (CB) are also shown. Numbers with side bullets indicate positions of molecular weight markers (in kDa).

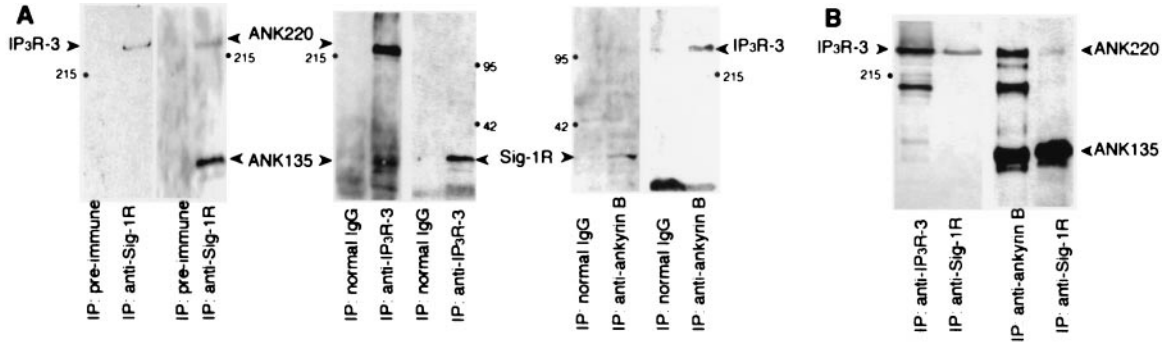

Fig. 2. Coupling of Sig-1R, ankyrin B, and IP_3R-3 as a trimeric complex. (*A*) Coimmunoprecipitation (IP) followed by Western blotting of the Sig-1R/ankyrin B/IP_3R-3 complex by respective cognate antibodies. (*B*) Percentages of IP_3R-3 and ankyrin B, respectively, coimmunoprecipitated with Sig-1R. IP_3R-3 were immunoprecipitated with anti-IP_3R-3 antibodies or anti-Sig-1R antibodies. Ankyrin B isoforms were coimmunoprecipitated with either anti-ankyrin B antibodies or anti-Sig-1R antibodies. Immunoblots were digitally scanned and densitometrically quantified by a Macintosh computer-based image analysis program (IMAGE, National Institutes of Health). Note: Anti-IP_3R-3 antibodies and anti-ankyrin B antibodies also immunoprecipitated proteolytic products of IP_3R-3 and ankyrin B, respectively (see lanes 1 and 3, from left).

Results

IP_3R-3 and Ankyrin B in NG-108 Cells. Immunoblottings by using specific antibodies indicated that NG-108 cells were predominantly expressing IP_3R-3 rather than IP_3R type 1 (Fig. 1). Isoforms of ankyrin B were detected in NG-108 cells (Fig. 1). Ankyrin G was not detected in NG-108 cells (Fig. 1).

The Sig-1R/Ankyrin B/IP_3R-3 Complex and Its Regulation by Sig-1R Agonists. First, we examined whether Sig-1R bind to the ankyrin/IP_3R-3 complex (7, 8, 34) in NG-108 cells. Sig-1R antibodies coimmunoprecipitated both IP_3R-3 and ankyrin B isoforms (e.g., ANK220, ANK135) in NG-108 cells (Fig. 2*A*). In analogy to that reported in rat brain (34), IP_3R-3 antibodies coimmunoprecipitated ankyrin B isoforms. However, ANK220 was the major isoform coimmunoprecipitated with IP_3R-3 and not ANK135 (Fig. 2*A*). IP_3R-3 antibodies also coimmunoprecipitated Sig-1R (Fig. 2*A*). The ankyrin B antibody coimmunoprecipitated Sig-1R and IP_3R-3 (Fig. 2*A*). Thus, Sig-1R form a multicomplex with ankyrin B and IP_3R-3 in NG-108 cells.

Percentages of the total IP_3R-3 and ankyrin B, which may exist in a complex with Sig-1R, were determined. About 43% of IP_3R-3 was coimmunoprecipitated with Sig-1R (Fig. 2*B*). About 20% of ANK220 was coimmunoprecipitated with Sig-1R (Fig. 2*B*). However, about 97% of ANK135 was coimmunoprecipitated with Sig-1R (Fig. 2*B*). The majority of ANK135 are thus coupled to Sig-1R, whereas only a portion of ANK220 is coupled to Sig-1R.

We examined next whether Sig-1R agonists like (+)pentazocine [(+)PTZ], (+)SKF10047, and PRE084 might affect the complex formation between Sig-1R, ankyrin B, and IP_3R-3. (+)PTZ treatment (100 nM, 10 min) caused ankyrin B isoforms, predominantly ANK220, to dissociate from IP_3R-3 (Fig. 3*A*). The ANK135 was not significantly affected (Fig. 3*A*). It took about 10 min for (+)PTZ to dissociate ≈70% of ANK220 from IP_3R-3 (Fig. 3*A*). The concentrations of (+)PTZ (low nM) in causing the ANK220 dissociation were close to the K_d value of (+)PTZ at Sig-1R (11) (Fig. 3*A*). The same results were obtained with PRE084 and (+)SKF10047 (Fig. 3*B*). NE-100, a high-affinity Sig-1R antagonist (35), although by itself not affecting the coimmunoprecipitation of ankyrin B with IP_3R-3 (Fig. 3*B*), blocked the ANK220 dissociation from IP_3R-3 caused by (+)PTZ (Fig. 3*C*).

Regulation of Ankyrin Levels in the P3L Fraction by Sig-1R and Associated Ligands. IP_3R are ER proteins (7, 8). Therefore, results from the above immunoprecipitation studies might suggest that

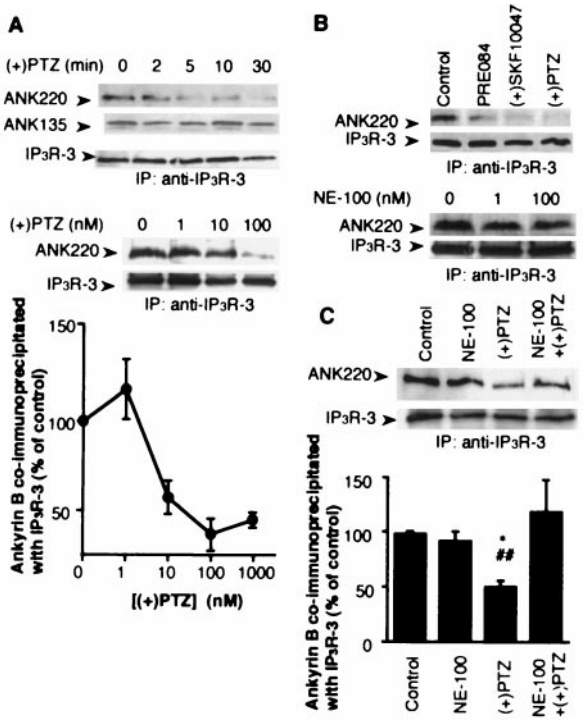

Fig. 3. Effects of Sig-1R ligands on the dissociation of ankyrin B (ANK220) from IP_3R-3 in NG-108 cells. NG-108 cells were incubated with respective drugs and then lysed for coimmunoprecipitation (IP) studies. (*A*) Time- and concentration-dependent dissociation of ankyrin B (ANK220) from IP_3R-3 by the (+)PTZ treatment. The concentration of (+)PTZ in the top row was 100 nM. For the concentration-dependent curve, immunoblots were digitally scanned and densitometrically analyzed by the National Institutes of Health IMAGE program. Data were normalized to total immunoprecipitated IP_3R-3 proteins and expressed as percentage relative to the level of coimmunoprecipitated ANK220 obtained in the absence of (+)PTZ. Note: Ten-minute treatment time for all concentrations. Data represent mean ± SEM from two to four separate determinations. (*B*) Effects of selective Sig-1R ligands on ANK220 coupling to IP_3R-3. Sig-1R agonists (100 nM, 10 min) decreased the amount of ANK220 coimmunoprecipitated with IP_3R-3 without altering the level of IP_3R-3. NE-100 (100 nM), a Sig-1R antagonist, did not by itself affect the ANK220 dissociation from IP_3R-3. (*C*) Inhibition of (+)PTZ-induced ANK220 dissociation from IP_3R-3 by NE-100. NE-100 (100 nM) was applied 5 min before (+)PTZ (100 nM, 10 min). Data were analyzed as described in *A* and represent mean ± SEM from six to seven separate determinations. *, $P < 0.05$ compared with ''control''; ##, $P < 0.01$ compared with ''NE-100 + (+)PTZ''.

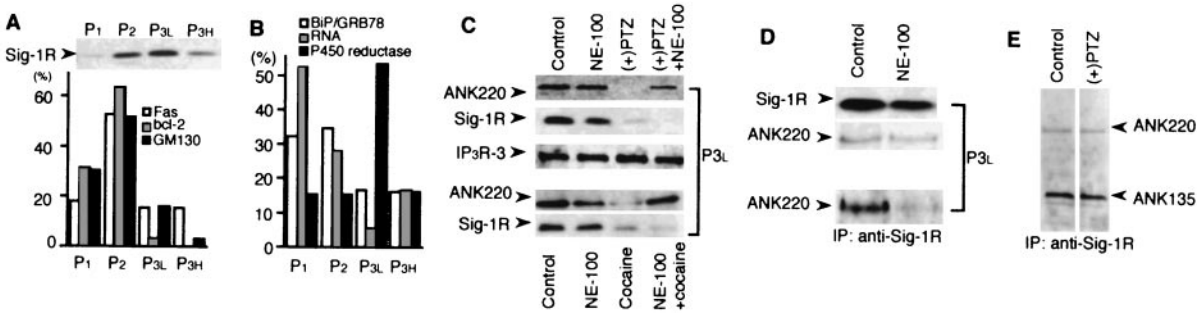

Fig. 4. Regulation of the level of ANK220 in the P3L fraction. (*A* and *B*) Distribution of Sig-1R (immunoblotting) and the relative enrichments of subcellular markers for the plasma membrane (Fas), mitochondria (bcl2), Golgi (GM130) (*A*), rough ER (BiP/GRB78 and RNA), and smooth ER (P450 reductase) (*B*) in the P1, P2, P3L, and P3H fractions (see *Methods*). The total density of each marker at the P1, P2, P3L, and P3H fractions from Western blotting were taken as 100%. (*C*) Top two and bottom two rows: NE-100 blocked the loss of ANK220, but not Sig-1R, caused by the (+)PTZ (100 nM, 10 min) or cocaine treatment (10 μM, 10 min). The IP_3R-3 levels remained unaltered under all conditions (middle row). (*D*) Effects of NE-100 treatment (100 nM, 15 min) by itself on the total levels of Sig-1R and ANK220 (top two rows) and on the portion of ankyrin B coimmunoprecipitated (IP) by anti-Sig-1R antibodies in the P3L fraction (lower row). (*E*) Effects of (+)PTZ treatment (100 nM, 10 min) on the ANK220 and ANK135 that could be coimmunoprecipitated by anti-Sig-1R antibodies in the whole cell lysate.

Sig-1R agonists can cause the dissociation of ANK220 from the ER. We thus examined the level of ANK220 in the P3L subcellular fraction (see *Methods*), which was characterized in this study and found to be enriched in Sig-1R and smooth ER with minimal contaminations from other organelles (Fig. 4 *A* and *B*).

The ANK220 level in the P3L fraction was reduced by the (+)PTZ treatment (Fig. 4*C*, Top Row). This effect by (+)PTZ was blocked by NE-100 (Fig. 4*C*, Top Row). Sig-1R were also reduced in the P3L fraction by (+)PTZ (Fig. 4*C*, Second Row). However, the Sig-1R loss from the P3L fraction caused by (+)PTZ was not blocked by NE-100 (Fig. 4*C*, Second Row). The levels of IP_3R-3 in the P3L fraction remained unaltered (Fig. 4*C*, Third Row). Because cocaine binds to Sig-1R (14) and because Sig-1R antagonists blocked the behavioral effects of cocaine (19, 20), the effects of cocaine were examined. Like (+)PTZ, cocaine also reduced the levels of both Sig-1R and ankyrin B in the P3L fraction (Fig. 4*C*, Lower Two Rows). NE-100 again blocked the ankyrin loss, but not the Sig-1R loss caused by cocaine (Fig. 4*C*, Lower Two Rows).

These results suggest that Sig-1R agonists cause the dissociation of ANK220, as well as Sig-1R, from the smooth ER. The results with NE-100, however, suggested that NE-100 may uncouple Sig-1R from the ANK220/IP_3R-3 complex, thus leaving (+)PTZ able to dissociate only Sig-1R from the ER. To provide evidence for this possibility, the effects of NE-100 alone were examined. NE-100 did not apparently affect the total ANK220 or total Sig-1R level in the P3L fraction (Fig. 4*D*, Top Two Rows). In the presence of NE-100, however, ANK220 could no longer coimmunoprecipitate with Sig-1R (Fig. 4*D*, Bottom Row). NE-100 may thus act as an "uncoupler" between ankyrin B and Sig-1R on the ER to achieve an apparent antagonistic effect against the pharmacological effects of Sig-1R agonists, such as (+)PTZ and cocaine.

It is interesting to note that the total amount of ANK220 (or ANK135) in NG-108 cells coimmunoprecipitated by anti-Sig-1R antibodies was found to be unaltered by the (+)PTZ treatment (Fig. 4*E*). This suggests that Sig-1R and ANK220 remain as a complex after dissociation from the ER.

ANK220 Dynamics Regulated by Sig-1R Affects Ca^{2+} Signaling at the IP_3R-3. We demonstrated previously that Sig-1R and associated ligands caused the potentiation of bradykinin-induced increase of cytosolic Ca^{2+} concentrations ($[Ca^{2+}]$cyt) in NG-108 cells without affecting IP_3 formation (30). Because ankyrin binding to IP_3R inhibited the IP_3R-mediated Ca^{2+} efflux (7, 8), the ankyrin dissociation from IP_3R-3 may, by extension, be related to Ca^{2+} efflux. Thus, we examined whether ankyrin dissociation from ER caused by Sig-1R ligands might affect $[Ca^{2+}]$cyt. $[Ca^{2+}]$cyt was monitored by using confocal microscopy.

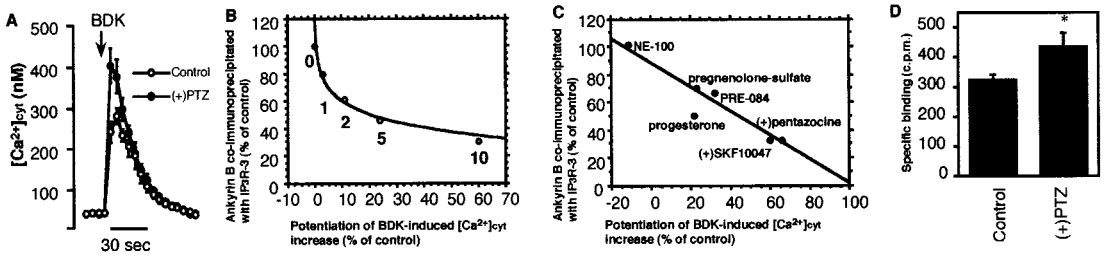

Fig. 5. Relationship between the degree of dissociation of ANK220 from IP_3R-3 induced by Sig-1R ligands and the Sig-1R ligands' abilities to potentiate bradykinin-induced increase in $[Ca^{2+}]$cyt in NG-108 cells. (*A*) Potentiation of the bradykinin-induced increase in $[Ca^{2+}]$cyt by (+)PTZ (100 nM, 10 min). (*B*) Temporal correlation of (+)PTZ (100 nM) in increasing the dissociation of ANK220 from IP_3R-3 and in potentiating the $[Ca^{2+}]$cyt increase induced by bradykinin. The numbers below open circles indicate the treatment time (min) of NG-108 cells with (+)PTZ. (*C*) Efficacy correlation of Sig-1R ligands in their abilities to cause ANK220 dissociation from IP_3R-3 at the 10-min point and in their abilities at the same time point to potentiate bradykinin-induced increases in $[Ca^{2+}]$cyt. Concentrations of Sig-1R ligands were all 100 nM. The total number of cells examined and the number of determinations (in parentheses) for each test drug are indicated (see *Methods*): NE-100, 23 cells (5); pregnenolone sulfate, 58 cells (7); progesterone, 34 cells (5); PRE084, 91 cells (14); (+)SKF-10047, 36 cells (6); (+)PTZ, 59 cells (8). The value on the *x* axis represents the mean value from all determinations for each drug. (*D*) Increase in $[^3H]IP_3$ binding to microsomes of NG-108 cells caused by (+)PTZ. After the (+)PTZ treatment (100 nM, 10 min), cells were harvested and P3 fractions prepared and used for $[^3H]IP_3$ binding assay. Data represent mean ± SEM of three determinations, each assayed in triplicate. *, $P < 0.05$.

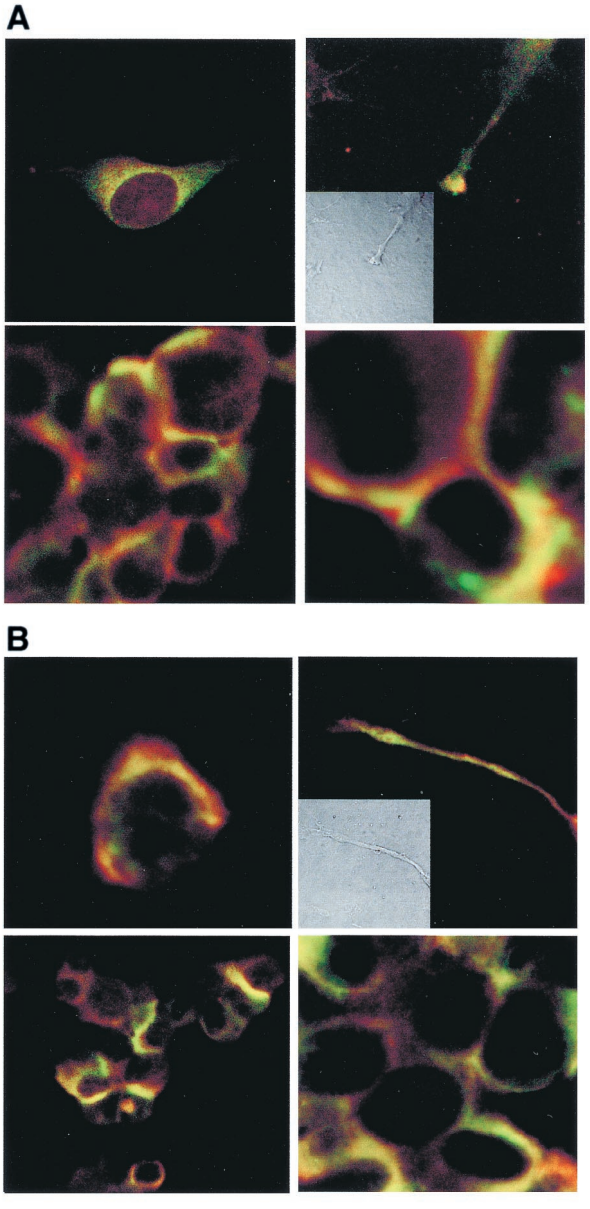

Fig. 6. Colocalization of ankyrin, IP_3R-3, and Sig-1R in NG-108 cells. (*A*) Immunocytohistochemical colocalization (yellow) of Sig-1R (green) and ankyrin B (red) in reticular perinuclear areas (*Top Left*), plasmalemmal regions of cell–cell contact (lower panels in low and high magnifications, respectively), and growth cones of processes in NG-108 cells (*Top Right*; *Inset*: Nomarski optical image). (*B*) Immunocytohistochemical colocalization (yellow) of Sig-1R (green) and IP_3R-3 (red) in perinuclear areas (*Top Left*), plasmalemmal regions of cell–cell contact (lower panels in low and high magnifications, respectively), and growth cones of processes in NG-108 cells (*Top Right*; *Inset*: Nomarski optical image).

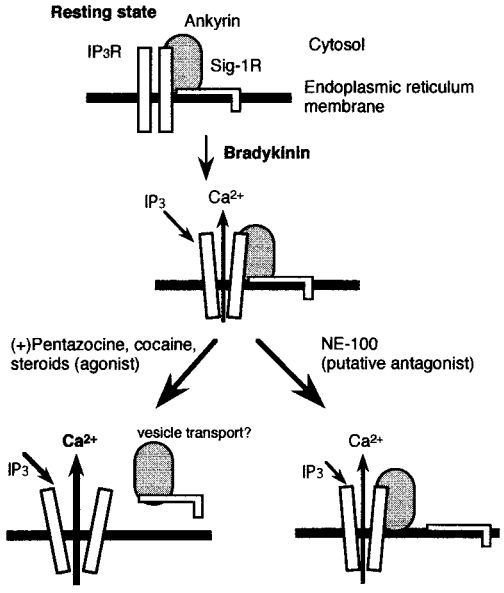

Fig. 7. Hypothetical diagram depicting the regulation of ANK220 by Sig-1R and associated ligands. In the presence of a Sig-1R agonist, such as (+)PTZ, cocaine, or certain steroids, the Sig-1R/ankyrin B complex dissociates from IP_3R-3 on the ER perhaps as a transport vesicle. As a result, IP_3 binding to IP_3R-3 increases and the Ca^{2+} efflux is enhanced. In the presence of the putative Sig-1R antagonist, NE-100, Sig-1R is dissociated from ANK220, which remains coupled to IP_3R on the ER.

It was found that, although Sig-1R ligands caused dissociation of ankyrin B, specifically ANK220 (see Fig. 3*A*), from IP_3R-3, the basal $[Ca^{2+}]$cyt was, in agreement with our previous results (30), not altered. This indicates that dissociation of ankyrin *per se* from IP_3R-3 does not open IP_3R-3 channels and that the low IP_3 concentration in resting cells is unable to trigger Ca^{2+} efflux from the ER. However, the results also suggest a possibility that, given a sufficient concentration of IP_3, the dissociation of ANK220 from IP_3R-3 may participate in the opening of IP_3R-3 channels. Because bradykinin is known to increase IP_3 (30, 36), and, because we have shown that Sig-1R ligands potentiate the bradykinin-induced increase in $[Ca^{2+}]$cyt (30), we examined whether the dissociation of ANK220 from IP_3R-3 caused by Sig-1R ligands may correlate with their potencies to potentiate the bradykinin-induced increase in $[Ca^{2+}]$cyt.

It took about 10 min for (+)PTZ to reach a near maximal effect in causing both the ANK220 dissociation and the $[Ca^{2+}]$cyt potentiation (Fig. 5 *A* and *B*). The efficacies of Sig-1R ligands, including certain steroids, to dissociate ANK220 from IP_3R-3 at the 10-min time point correlated excellently with their abilities to potentiate the bradykinin-induced increase in $[Ca^{2+}]$cyt (Fig. 5*C*; $r = 0.938$; $P = 0.0057$).

To demonstrate a causal link behind these effects, we examined next whether (+)PTZ, by causing a dissociation of ANK220 from IP_3R-3, may increase the binding of $[^3H]IP_3$ to IP_3R, thus causing an increase in Ca^{2+} efflux. Indeed, $[^3H]IP_3$ binding to ER membrane was increased by about 30% in (+)PTZ-treated cells (Fig. 5*D*). Thus, the dissociation of ANK220 from IP_3R-3 caused by Sig-1R agonists enhances the interaction between IP_3 and IP_3R-3, leading to a potentiation of the bradykinin-induced increase in $[Ca^{2+}]$cyt.

Colocalization of Sig-1R, Ankyrin B, and IP_3R-3. Immunocytohistochemistry indicates that ankyrin B and Sig-1R are colocalized in certain areas in NG-108 cells. Specifically, colocalization is seen in perinuclear areas in reticular patterns (Fig. 6 *A* and *B*). In confluent cells, striking colocalizations are seen in plasmalemmal regions of cell–cell contact (Fig. 6*A*). Moreover, Sig-1R and ankyrin are also colocalized in growth cones (Fig. 6*A*). Sig-1R are also colocalized with IP_3R-3 in the same areas where Sig-1R and ankyrins are colocalized (Fig. 6*B*). In particular, growth cones exhibit the colocalization of Sig-1R and IP_3R-3 (Fig. 6*B*). These results support the presence of the Sig-1R/ankyrin B/IP_3R-3 complex at the ER and in cellular components implicated in cell-to-cell interaction and cell growth.

Discussion

Sig-1R modulate neurotransmitter release (37), synaptic activity (38), contraction of cardiac myocytes (27, 28), and learning and

memory (18). Sig-1R contain a putative transmembrane region at the N-terminal and two stretches of hydrophobic amino acids (22). It has been suggested that Sig-1R and similar putative one-transmembrane ER proteins may serve to anchor other proteins to the membrane surface (22, 39). Here, we demonstrate that Sig-1R represent unique one-transmembrane proteins that not only anchor ankyrins to the ER membrane, but also modulate the function of ankyrin at the IP_3R-3 on the ER in an apparent agonist–antagonist fashion (see Fig. 7). Ankyrin translocates from ER along microtubles, thus playing an important role in vesicle transport (5). Sig-1R agonists may thus modulate vesicle transport and neurotransmitter release by affecting the dynamics of ankyrin. Sig-1R agonists may exert such action by facilitating the vesicular transport processes enclosing Sig-1R as the transmembrane cargo proteins and ankyrins as the coat or adapter proteins.

The possibility that a direct binding of Sig-1R agonist to ankyrin may occur cannot be totally excluded in the present study. However, the direct binding, if any, cannot explain the Ca^{2+} mobilization caused by Sig-1R agonists. The selective Sig-1R antagonist NE-100 can block the action of Sig-1R agonists (30). Also, structurally diverse Sig-1R agonists such as (+)PTZ, pregnenolone sulfate, and PRE084 all elicited Ca^{2+} signaling, which may only be best explained by their interaction with Sig-1R.

Although Sig-1R are coupled to both ANK220 and ANK135 in NG-108 cells (Fig. 2*B*), (+)PTZ appeared to predominantly dissociate ANK220 from IP_3R-3 and not ANK135 (Fig. 3*A*). However, (+)PTZ caused a reduction of both ANK220 and ANK135 from the P3 fraction (data not shown). These results suggest that the majority of the Sig-1R/ANK135 complex in the P3 fraction is not coupled to IP_3R-3 and that the Sig-1R/ANK220 and Sig-1R/ANK135 complexes, respectively, may play different physiological roles. The Sig-1R/ANK220 complex may regulate the function of IP_3R-3, as demonstrated in this study. The exact function of the Sig-1R/ANK135 is unknown at present. A small cytosolic ankyrin isoform was suggested to be related to a network of subcellular organelles and protein transport (5, 40). Whether Sig-1R/ANK135 may participate in such functions is unknown.

Sig-1R may thus play important roles in functions previously recognized to be associated with ankyrin B. These roles of Sig-1R might be achieved by binding of Sig-1R ligands or by an increase in the concentrations of Sig-1R-binding steroids in response to stress or the menstrual cycle (41). Finally, because Sig-1R have been implicated in actions of certain psychotropic drugs including cocaine (12–14, 19, 20, 42, 43), further understanding of the ankyrin B dynamics regulated by Sig-1R may pave a new avenue in psychopharmacology linking certain actions of psychotropic drugs to the dynamics and functions of cytoskeletal proteins.

This study was supported by the Intramural Research Program of National Institutes on Drug Abuse, National Institutes of Health and in part by the Division of Basic Research, National Institutes on Drug Abuse, and the Pharmacopsychiatry Re-search Foundation of Japan.

1. Bennett, V. & Stenbuck, P. J. (1979) *Nature (London)* **280,** 468–473.
2. Bennett, V. (1979) *Nature (London)* **281,** 597–599.
3. Nelson, W. J. & Veshnock, P. J. (1987) *Nature (London)* **328,** 533–536.
4. Srinivasan, Y., Elmer, L., Davis, J., Bennett, V. & Angelides, K. (1988) *Nature (London)* **333,** 177–180.
5. De Matteis, M. A. & Morrow J. S. (1998) *Curr. Opin. Cell Biol.* **10,** 542–549.
6. Tuvia, S., Buhusi, M., Davis, L., Reedy, M. & Bennett, V. (1999) *J. Cell Biol.* **147,** 995–1007.
7. Bourguignon, L. Y. & Jin, H. (1995) *J. Biol. Chem.* **270,** 7257–7260.
8. Bourguignon, L. Y., Jin, H., Iida, N., Brandt, N. R. & Zhang, S. H. (1993) *J. Biol. Chem*. **268,** 7290–7297.
9. Martin, W. R., Eades, C. E., Thompson, J. A., Huppler, R. E. & Gilbert, P. E. (1976) *J. Pharmacol. Exp. Ther.* **197,** 517–532.
10. Zukin, S. R. & Zukin, R. S. (1979) *Proc. Natl. Acad. Sci. USA* **76,** 5372–5376.
11. Quirion, R., Bowen, W. D., Itzhak, Y., Junien, J. L., Musacchio, J. M., Rothman, R. B., Su, T. P., Tam, S. W. & Taylor, D. P. (1992) *Trends Pharmacol. Sci.* **13,** 85–86.
12. Largent, B. L., Gundlach, A. L. & Snyder, S. H. (1984) *Proc. Natl. Acad. Sci. USA* **81,** 4983–4987.
13. Snyder, S. H. & Largent, B. L. (1989) *J. Neuropsychiatry* **1,** 7–15.
14. Sharkey, J., Glen, K. A., Wolfe, S. & Kuhar, M. J. (1988) *Eur. J. Pharmacol.* **149,** 171–174.
15. Su, T.-P., London, E. D. & Jaffe, J. H. (1988) *Science* **240,** 219–221.
16. Tam, S. W. (1983) *Proc. Natl. Acad. Sci. USA* **80,** 6703–6707.
17. Graybiel, A. M., Besson, M.-J. & Weber, E. (1989) *J. Neurosci.* **9,** 326–338.
18. Maurice, T., Su, T.-P. & Privat, A. (1998) *Neuroscience* **83,** 413–428.
19. McCracken, K. A., Bowen, W. D., de Costa, B. R. & Matsumoto, R. R. (1999) *Eur. J. Pharmacol.* **16,** 225–232.
20. Maurice, T., Romieu, P. & Martin-Farden, R. (2000) *Soc. Neurosci.* **26,** 526.
21. Su, T.-P. (1991) *Eur. J. Biochem.* **200,** 633–642.
22. Hanner, M., Moebius, F. F., Flandorfer, A., Knus, H-G., Striessnig, J., Kempner, E. & Glossmann H. (1996) *Proc. Natl. Acad. Sci. USA* **93,** 8072–8077.
23. Labit-Le Bouteiller, C., Jamme, M. F., David, M., Silve, S., Lanau, C., Dhers, C., Picard, C., Rahier, A., Taton, M., Loison, G., *et al.* (1998) *Eur. J. Biochem.* **256,** 342–349.
24. Brent, P. L., Herd, L., Saunders, H., Sim, A. T. R. & Dunkley, P. R. (1997) *J. Neurochem.* **68,** 2201–2211.
25. Hayashi, T., Kagaya, A., Takebayashi, M., Shimizu, M., Uchitomi, Y., Motohashi, N. & Yamawaki, S. (1995) *J. Pharmacol. Exp. Ther.* **275,** 207–214.
26. Klette, K. L., Lin, Y., Clapp, L. E., DeCoster, M. A., Moreton, J. E. & Tortella, F. C. (1997) *Brain Res.* **756,** 231–240.
27. Ela, C., Barg, J. Vogel, Z., Hasin, Y. & Eilam, Y. (1994) *J. Pharmacol. Exp. Ther.* **269,** 1300–1309.
28. Novakova, M., Ela, C., Bowen, W. D., Hasin, Y. & Eilam, Y. (1998) *Eur. J. Pharmacol.* **353,** 315–327.
29. Tsao, L.-I. & Su, T.-P. (1996) *Eur. J. Pharmacol.* **311,** R1–R2.
30. Hayashi, T., Maurice, T. & Su, T.-P. (2000) *J. Pharmacol. Exp. Ther.* **293,** 788–798.
31. Seth, P., Fei, Y. J., Li, H. W., Huang, W., Leibach, F. H. & Ganapathy, V. (1998) *J. Neurochem.* **70,** 922–931.
32. Steer C. J., Klausner, R. D. & Blumenthal, R. (1982) *J. Biol. Chem.* **257,** 8533–8540.
33. Su, T.-P., Wu, X-Z, Cone, E. J., Shukla, K., Gund, T., Dodge, A. L. & Parish, D. W. (1991) *J. Phamacol. Exp. Ther.* **259,** 543–550.
34. Joseph, S. K. & Samanta, S. (1993) *J. Biol. Chem.* **268,** 6477–6486.
35. Okuyama, S. & Nakazato, A. (1996) *Cent. Nerv. Syst. Drug Rev.* **2,** 226–237.
36. Berridge, M. J. (1993) *Nature (London)* **361,** 315–325.
37. Matsuno, K., Matsunaga, K., Senda, T. & Mita, S. (1993) *J. Pharmacol. Exp. Ther.* **265,** 851–859.
38. Monnet, F. P., Debonnel, G. & de Montigny, C. (1992) *J. Pharmacol. Exp. Ther.* **261,** 123–130.
39. Keon, J. P., James, C. S., Court, S., Baden-Daintree, C., Bailey, A. M., Burden, R. S., Bard, M. & Hargreaves, J. A. (1994) *Curr. Genet.* **25,** 531–537.
40. Devarajan, P., Stabach, P. R., Mann, A. S., Ardito, T., Kashgarian, M. & Morrow, J. S. (1996) *J. Cell Biol.* **133,** 819–830.
41. Baulieu, E. E. (1998) *Psychoneuroendocrinology* **23,** 963–987.
42. Ferris, C. D., Hirsch, D. J., Brooks, B. P. & Snyder, S. H. (1991) *J. Neurochem.* **57,** 729–737.
43. Kahoun, J. R. & Ruoho, A. E. (1992) *Proc. Natl. Acad. Sci. USA* **89,** 1393–1397.